

# Glass Confidence Maps Building Based on Neural Networks Using Laser Range-finders for Mobile Robots

Jun Jiang, Renato Miyagusuku, Atsushi Yamashita, and Hajime Asama

**Abstract**—In this paper, we propose a method to classify glass and non-glass objects and build glass confidence maps for indoor mobile robots using laser range-finders (LRFs). The glass confidence map is aimed to improve robot localization systems’ robustness and accuracy in glass environments. For most LRF-based localization systems, objects are assumed to be detectable from all incident angles, which is true for non-reflective and non-transparent objects, like walls. However, glass can only be detected by LRFs in certain incident angles. This glass detection failure decreases robots’ localization accuracy. Exhibiting glass’ position in the map and taking its detection failure into consideration can increase the localization accuracy. We propose the usage of a neural network to classify glass and non-glass objects, with LRF’s measured intensity, distance and incident angles as inputs. We verified our method experimentally, and experimental results show that our method can successfully distinguish glass from non-glass objects and accurately construct a glass confidence map with high confidence.

## I. INTRODUCTION

There is high potential for the usage of mobile robots in human environments like homes, shopping malls and offices. For these robots, localization is an essential task, and because glass is very common in the above-mentioned environments, as shown in Fig. 1, being able to localize robustly in glass environments is important. In this paper, we propose a method aiming to improve the robustness of mobile robots’ localization systems in indoor human environments.

A lot of current popular localization systems for mobile robots are based on Laser Range-finders (LRFs), because of their high accuracy measuring distance. However, LRF-based localization systems perform unsatisfyingly in glass environments [1]. By default, objects are assumed to be detectable in all incident angles, but glass is only detectable to LRFs for small incident angles. This glass detection failure disturbs the existing scan matching schemes [2], and consequently negatively influences localization accuracy. A possible solution to this problem is to provide to the robot a ‘glass map’ of the environment, which shows if objects are glass or non-glass. Then the robot can take the LRFs’ glass detection failure into consideration when scanning glass objects. However, glass maps are rarely available, and manually making glass maps is not trivial. In order to solve this problem, in this paper we propose a method to classify

This work was partly funded by Tough Robotics Challenge, ImPACT Program of the Council for Science, Technology and Innovation (Cabinet Office, Government of Japan).

J. Jiang, R. Miyagusuku, A. Yamashita, and H. Asama are with the Department of Precision Engineering, Graduate School of Engineering, The University of Tokyo, Japan. {jiang, miyagusuku, yamashita, asama}@robot.t.u-tokyo.ac.jp



Fig. 1. Example of an indoor environment. Typically, glass are present in the surroundings.

glass and non-glass objects using laser range-finders (LRFs) and build glass confidence maps.

In order to build a glass map, the challenging point is to classify glass and non-glass objects, which has been previously explored by the robotics community. Lei et al. [3] proposed a method to detect transparent objects based on color images and LRF scan data. Lysenkov et al. [4] presented an approach to recognize transparent objects with a Kinect sensor. However, using multiple sensors may lead to calibration problems. Contrary to these approach, ours uses a LRF, considering LRFs are the most widely used sensors in robot localization and mapping. Recent work brought some progress to classifying glass and non-glass objects only using a LRF. Koch et al. [5] detected glass and classified glass and non-glass objects using a multi-echo LRF. However, their method requires using this special type of LRFs and cannot be applied to the more widely used single-echo LRFs. Our method does not have this restriction and can work on single-echo LRFs. Wang et al. [6] detected glass using the intensity change of specular reflection of the glass surface, which can also be used to classify glass and non-glass objects, although classification was not their focus. However, in order to receive the specularly reflected light, their method requires the robot to move in paths that enable it to scan objects from close to 0 deg of incident angle. Our method does not have this restriction and can detect glass in a larger range of incident angles.

In this paper, we propose a novel method to classify glass and non-glass objects using only a single LRF, and to build a glass confidence map. The proposed classifier is based on a 4-layer neural network and employs (i) LRF measured

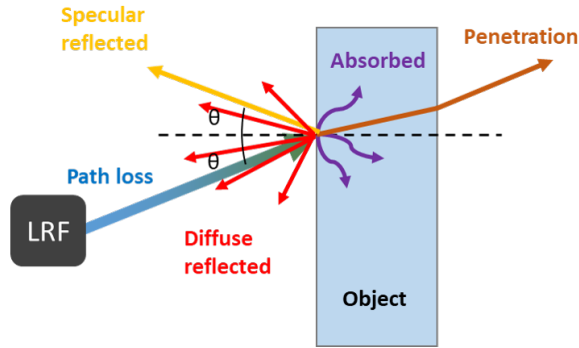


Fig. 2. Physical phenomena during the LRF scanning process.

distance, (ii) intensity and (iii) corresponding incident angle as inputs. It can work on common LRFs, and do not have strict restrictions on the scanning incident angle. In addition, the proposed glass confidence map is a grid map exhibiting both objects' positions and their probabilities of being glass. Grid map representation and a probabilistic approach are chosen to build the glass map, because they are widely used in robot localization, and can thus be helpful for ease of integrating our method with common localization algorithms.

The rest of this paper is organized as follows: Section II provides related physical theories, and Section III includes an overview of our proposed method, and primary experimental verification results. Section IV presents the details of our proposed neural network based classifier. Section V includes system structure and algorithm of using our proposed method to build a glass confidence map. Section VI shows experimental results of glass map building in an indoor environment. Finally, conclusions and future works are drawn in Section VII.

## II. LRF PRINCIPLES AND RELATED PHYSICS

A LRF scans an environment by sending out multiple beams of laser light sequentially in a fan shape, and then waiting for the light being reflected back to it by objects. By measuring the time of flight of the laser beams, the LRF can calculate the distance to the objects in the environment.

As shown in Fig. 2, when propagating through space, LRF's emitted laser loses part of its energy. The ratio of lost energy in its path is determined by the distance and medium. When it hits an object, the laser goes through three main physical phenomena: (i) penetration (mainly determined by object's transparency); (ii) reflection (determined by the object's reflective index, incident angle, as well as incident light wavelength and polarization); and (iii) absorption of the remaining light. Among these three parts, only the reflected part might be received by the LRF. Moreover, light can be reflected in two ways, diffusely reflected and specularly reflected, determined mainly by the surface's roughness and micro-structure. If the LRF scans at 0 deg of incident angle, both types of reflected light may return to the LRF, if else, only part of the diffuse reflection can return to the LRF. Because the diffuse reflection intensity is not even in each

direction, incident angle also makes a big difference. Finally, after going through another path loss, the reflected laser goes back to the LRF. However, the intensity value we get from the LRF is not the true intensity of the returned laser. The effect of LRF signal processing mechanism, which differs for different models, has also to be taken into consideration.

Although there are many influencing factors in the LRF scanning process, in the case of mobile robots, factors related to LRF model and medium can be considered fixed, and the rest can be simplified into three main factors, material  $m$ , distance  $d$  and incident angle  $\theta$ . Glass and non-glass objects have obviously different material features, such as transparency, roughness, and reflective index, thus their LRF received intensities should be different when other factors are the same. Therefore, theoretically, glass and non-glass objects can be classified based on their LRF intensities, considering the influence of distance and incident angle.

## III. CLASSIFICATION METHODOLOGY

In this section, firstly, an overview of our proposed classification method is given based on the analyses in the last section. Then the feasibility of this method is primarily examined through experiments. At the end, about how to build the proposed classifier is discussed based on the experiment results.

### A. Classifier Overview

Based on the physical analyses in the last section, an object's LRF intensities is mainly determined by its material type, distance and incident angle, hence its material type can be reflected by these three factors. In fact, Kirchner et al. [7] used a simpler but similar method to classify common opaque materials, such as wood and cloth. In their research, distance is assumed to be fixed and materials are classified based on the relationship of intensity and incident angle. In other words, they built the following mapping function, where  $m$  means material type, under the condition that distance  $d$  is a constant value:

$$f(I, \theta) \rightarrow m. \quad (1)$$

However, their method is insufficient to solve the classification problem mentioned in this paper. Because, first, their method is only verified on opaque materials, not covering any transparent object like glass; and second, distance changes significantly in the case of mobile robots, and thus cannot be assumed to be fixed.

In order to build a more suitable mapping function to classify glass and non-glass for mobile robots, in this paper, we take distance's influence into consideration and propose to build the following extended mapping function from LRF measured intensity  $I$ , LRF measured distance  $d$ , and corresponding incident angle  $\theta$  to material type  $m$  (glass or non-glass):

$$f(I, d, \theta) \rightarrow m. \quad (2)$$

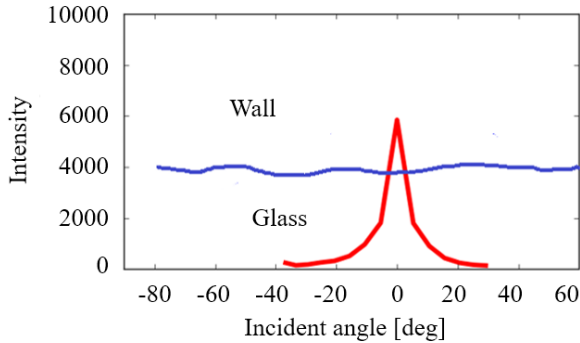


Fig. 3. Comparison of the relationship of intensity and incident angle between white walls and glass.

### B. Primary Experimental Verification

In order to verify that glass and non-glass object can be classified based on intensity, distance and incident angle, we performed two simple experiments. In order to decrease complexity as well as investigate the influence of each factor, in each experiment we measured intensities fixing either distance or incident angle, while varying the other one, for both glass and non-glass samples. For both experiments, we used a Hokuyo UTM 30LX-EW LRF. It has to be noted that although the LRF we used is a multi-echo LRF, our method does not need its multi-echo function and can work on common LRFs. In the experiments we only use the first echo.

In the first experiment, we scanned a glass and a white wall from different angles, with distance fixed at 1 m. According to the results shown in Fig. 3, glass and wall have totally different curve shapes and can be easily distinguished. Glass has lower intensities or even becomes undetectable at large incident angles, which matches theories because its transparency is so high that most of light penetrates. Besides, its roughness is relatively low, and thus the reflection is mainly specular, which leads to that the intensity near 0 deg is extremely high. The wall tested in our experiment shows nearly uniform intensities at any incident angle, which might be because it is a nearly ideal matte surface.

In the second experiment, we scanned the same samples at different distances, with incident angle fixed at near 0 deg. The results are shown in Fig. 4. Results show that glass and wall can be easily distinguished based on their intensities in near distances. While as distance increases, glass data becomes highly noisy and sparse, increasing the difficulties of classification. It is worth to note that according to inverse-square law [8], intensity should decrease monotonously as distance increases. However, experimental results show intensity peaks at near 1 m for all materials. We consider that this discrepancy between theory and practice results from the LRF's signal processing mechanism, which means that using LRF intensity to classify has limitation related to used LRF models.

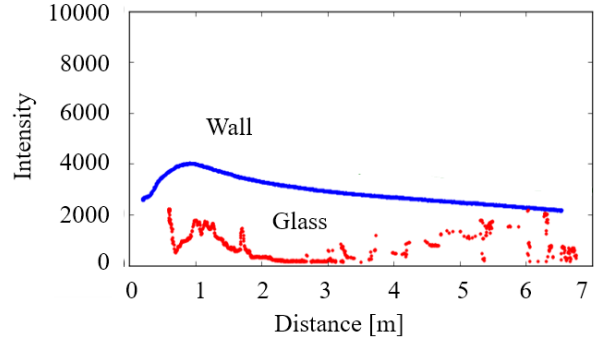


Fig. 4. Comparison of the relationship of intensity and distance between white walls and glass at 0 deg of incident angle.

### C. Classifier Building Methods

In the primary validation experiments mentioned before, we had one factor fixed at each time. However, in practice, both distance and incident angle change at the same time as the robot moves. Therefore, it is necessary to consider all changing factors jointly.

Kirchner et al. [7] proposed a classification method based on fitting intensity to a second degree polynomial function of incident angle. If we want to use a similar approach, given our assumption, we would have to find a mapping function that also consider distance. However, when considering the change of incident angle and distance jointly, finding an explicit mapping function turns out to be impractical because of the following reasons:

- The distance-intensity relationship is non-linear and varies for different materials.
- Theory does not match practice because of LRFs' signal processing mechanism, which are unclear and different for different models.
- Glass intensity data is noisy, increasing the difficulty of accurately building a function based on experiment data.

As results, to build the classifier, we choose to learn directly from data without an explicit model using machine learning methods.

## IV. CLASSIFIER BASED ON NEURAL NETWORKS

We choose to use a neural network to classify glass and non-glass objects after trying several types of common machine learning methods. Details of our proposed neural network are presented in the next sub-sections.

### A. Structure

We build a 4-layer neural network, including 1 input layer, 2 hidden layers and 1 output layer, as shown in Fig. 5. The input layer has 3 input nodes, which take a scalar value of intensity, incident angle and distance respectively. The 2 hidden layers both have 100 hidden nodes. The neural network with these certain numbers of hidden layers and hidden nodes performed best among various other structures

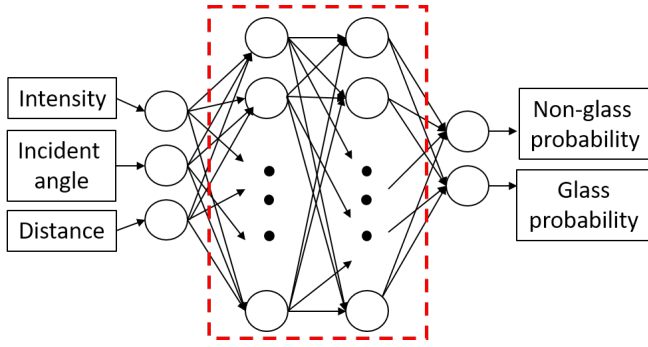


Fig. 5. Structure of the neural network. Hidden layers are in the red dash line box

we tried. Finally, the output layer includes 2 nodes, giving the probability of being glass and non-glass respectively. We used the Softmax function to normalize the probability to sum to 1.

### B. Training and Testing

We collected and labeled training data manually in the corridor shown in Fig. 1. Each training sample included a intensity and a distance value output by the LRF, as well as the corresponding incident angle of the scan, as shown in Fig. 6 (a). If the sample is glass, the probability of non-glass and glass are set to 0 and 1 respectively, if not, to 1 and 0. Our dataset included about 13,000 non-glass samples and 5700 glass samples. We used 80% of it for training, and 20% for testing. In testing, if the output probability of being glass was higher than 0.5, the sample was labeled as glass, and if not, as non-glass. Testing results showed that the trained neural network could reach a correct predicting rate of 97.3%.

### C. Prediction

A LRF scans in a fan shape and emits multiple beams in various directions. As a robot moves, a single point on a object surface (or a grid in the map) is usually scanned for multiple times (Fig. 6 (b)), generating multiple input samples. We input the samples into the trained neural network separately and get multiple probabilities for the same point. We calculated the final probability for this point by averaging all the output probabilities.

## V. GLASS CONFIDENCE MAP BUILDING

In previous sections, the details of our proposed classification method is presented. In this section, the system structure and algorithm of using our method to build a glass confidence map are described.

### A. System Structure

Our proposed classifier needs the (i) intensity  $I$ , (ii) distance  $d$  and (iii) incident angle  $\theta$  as inputs. Consequently, our proposed method needs to be input, first, LRF scan data, which provides  $I$  and  $d$ ; and second, the occupancy grid map of the environment and the robot position, from which  $\theta$  can be calculated. Our aim is to build a glass grid map showing

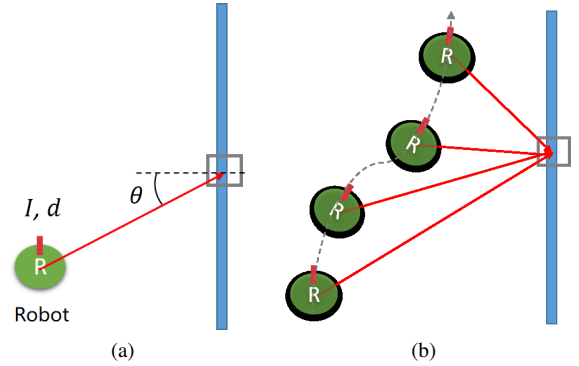


Fig. 6. (a) One sample includes a intensity  $I$ , a distance  $d$ , and the corresponding incident angle  $\theta$ . (b) A single point on a object surface (or a grid in a map) will be scanned for multiple times, generating multiple input samples.

each grid is glass or non-glass and add this information to the occupancy map.

In detail, the data processing flow chart of our system is shown in Fig. 7. Input data, which is shown in blue color, including robot odometry, LRF data and a normal occupancy grid map without object type information are input into both a localization algorithm and our proposed algorithm. The localization algorithm calculates the robot position in the occupancy map, which is also input into our proposed algorithm. Incident angles of each scan are calculated based on the robot pose and the occupancy grid map. Finally, a glass grid map of the environment is generated by our algorithm.

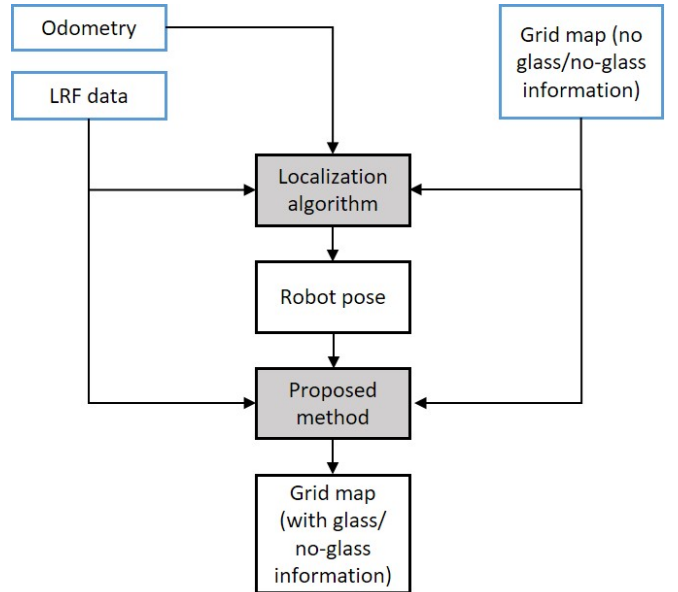


Fig. 7. Data processing flow chart of our implementation. Input data are shown in blue color. Blocks without background color are data, and blocks with background color are algorithms.



Fig. 8. A Pioneer 3-DX equipped with a Hokuyo UTM 30LX-EW LRF is used in the experiment

### B. Algorithm

Our proposed method builds the map using the procedure as follows:

- For each robot pose, find the chronologically nearest LRF scan, and perform the following steps.
- For each occupied grid in the map, find its surface normal, and then calculate the incident angle  $\theta$  based on the robot position and grid position.
- Locate beams in the direction of the target grid based on the robot pose and the grid position. Remove noise of the located beams by comparing the their measured distances and the calculated distances in the map. Calculate the mean intensity  $I$  and distance  $d$  of the filtered beams.
- Input  $\theta$ ,  $I$ ,  $d$  into the neural network and get the glass probability for the corresponding grid.
- Average all probabilities for the same grid generated at different robot pose, and then show the value in colors at corresponding positions in the glass confidence map.

## VI. EXPERIMENT

We performed an experiment to demonstrate the feasibility of our proposed method. As shown in Fig. 8, we fixed a Hokuyo UTM 30LX-EW LRF on a mobile robot, the Pioneer 3-DX, and tele-operated the robot along a corridor. In the corridor a large area of glass exits, as shown in Fig. 1. We recorded the robot’s odometry data and LRF scan data and obtained a normal occupancy grid map with glass marked as occupied grids using method proposed in [9]. Finally, we built a glass grid map with glass/non-glass information of each grid through the processing process shown in Fig. 7.

Figure 9 shows the normal occupancy grid map, where glass is marked manually, and the robot path and start position are shown in blue line and red dot respectively in the map. Figure 10 is the glass confidence map generated by our proposed method, which shows that our methods can classify glass and non-glass objects successfully. Not only wall, but also plastic trash bins and painted doors are all correctly classified as non-glass objects. Additionally, it has to be noted that part of the glass behind several trash bins is

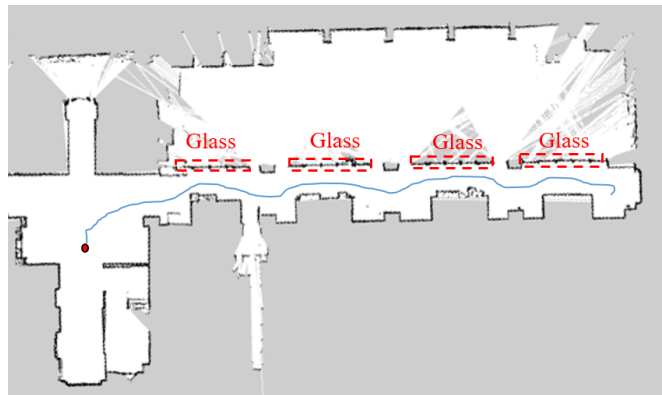


Fig. 9. Grid map of the experiment environment. The robot’s moving trace is marked in blue line, and the red dot is start position.

TABLE I  
CLASSIFICATION RESULTS

Material type	Glass	Non-glass
Total grid number	496	3854
Correct number	412	3783
Incorrect number	84	71
Correct rate	83 %	98 %

also correctly classified, as shown in Fig. 10 (e). This proves that our method does not require the object being scanned at the surface normal, showing advantage over the method proposed in [6].

Table I is classification results, according to which, 98% of non-glass grids and 83% of glass grids are correctly classified. Mis-classifications are mainly near to thin metallic pillars shown in Fig. 10 (c). Possible reasons for these mis-classifications include: first, the unpainted metallic pillars are shiny and reflective, and thus have similar reflective features as glass; second, robot localization errors affect strongly when encountering small-size objects, like the metallic pillars in our experiment; and third, glass near to the metallic pillars are more likely to be scanned with opaque objects right behind it, causing the intensity measured by the LRF are mainly from the opaque objects. Besides the mid-classifications near to the metallic pillars, another obvious failure is a glass door at the end of a long and narrow passage, shown in Fig. 10 (b), which is completely classified as non-glass objects. Possible reason for this failure is that the robot could not get enough scan samples because of its location.

Figure 11 is the probability histogram of the grids classified as glass. 62% of the glass grids have probabilities higher than 0.9, and 80% higher than 0.8. This result shows that most of the glass grids are classified with high confidence. It is worth to mention that because the training set was collected at a similar corridor with the experiment environment, potential over-fitting problems exist. However, we leave increasing the algorithm’s robustness for future work.

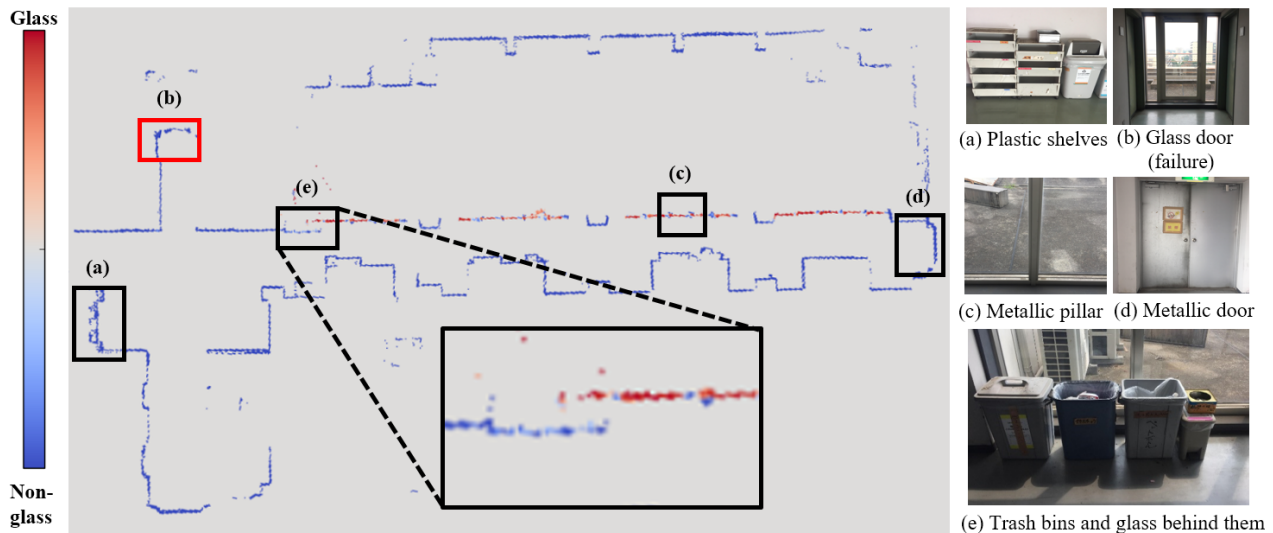


Fig. 10. The glass confidence map of the corridor built by our proposed method. Thin metallic pillar in (c) is correctly detected. Also, glass behind the trash bins in (e) is also detected.

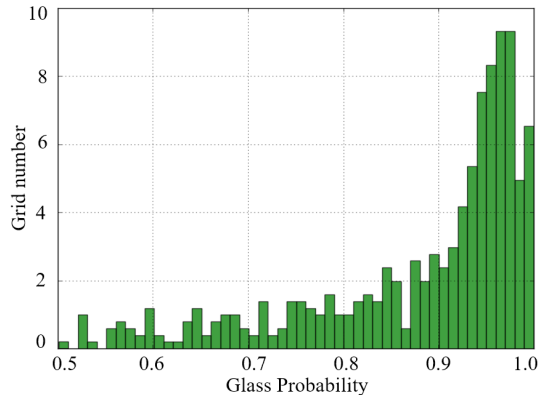


Fig. 11. Probability histogram of the grids classified as glass

## VII. CONCLUSIONS AND FUTURE WORK

In this paper, aiming to improve LRF-based robot localization systems' robustness, we proposed a novel approach to classify glass and non-glass objects and to build a glass confidence map, which can be used to solve the inaccurate localization problem caused by LRF glass detection failure. In order to minimum the limitations on used sensors, our method makes full use of the information, both distance and intensity, gathered by a single normal LRF. Also, our method adopts to use a neural network which serves to relaxing the requirements on scanning incident angle, allowing the robot's moving path to be freer.

To verify the feasibility of proposed solution, we performed an experiment to build a glass confidence map in a indoor environment. Experiment results show that the proposed method can successfully distinguish various kinds of non-glass objects from glass and build a glass confidence map with high confidence.

As future works, we wish to extend our method to manage

the possible causes of classification failures mentioned in the previous sections, and further test our method in various glass environments. Also, we'd like to enable our implementation to run online. Although our implementation runs off-line currently, it is possible to transfer our method into running online, as the information needed, including (i) LRF scan data, (ii) occupancy grid map and (iii) robot position in the map, can all be provided by a online glass-detectable SLAM algorithm. We also interested in integrating our method with a localization algorithm and then evaluating the localization accuracy improvement using our method.

## REFERENCES

- [1] J. Kim and W. Chung, "Localization of a mobile robot using a laser range finder in a glass-walled environment", *IEEE Transactions on Industrial Electronics*, vol. 63, no. 6, pp. 3616–3627, 2016.
- [2] C. Moon, W. Chung, and N. L. Doh, "Observation likelihood model design and failure recovery scheme toward reliable localization of mobile robots", *International Journal of Advanced Robotics Systems*, vol. 7, no. 4, pp. 113–122, 2010.
- [3] Z. Lei, K. Ohno, M. Tsubota, E. Takeuchi, and S. Tadokoro, "Transparent object detection using color image and laser reflectance image for mobile manipulator", in *Proceedings of the 2011 IEEE International Conference on Robotics and Biomimetics (ROBIO 2011)*, pp. 1–7, 2011.
- [4] I. Lysenkov, V. Eruhimov, and G. Bradski, "Recognition and pose estimation of rigid transparent objects with a kinect sensor", in *Proceedings of Robotics: Science and Systems*, pp. 1–8, 2012.
- [5] R. Koch, S. May, P. Murmann, and A. Nüchter, "Identification of transparent and specular reflective material in laser scans to discriminate affected measurements for faultless robotic slam", *Robotics and Autonomous Systems*, vol. 87, pp. 296–312, 2017.
- [6] X. Wang and J. Wang, "Detecting glass in simultaneous localisation and mapping", *Robotics and Autonomous Systems*, vol. 88, pp. 97–103, 2017.
- [7] N. Kirchner, D. Liu, and G. Dissanayake, "Surface type classification with a laser range finder", *IEEE Sensors Journal*, vol. 9, no. 9, pp. 1160–1168, 2009.
- [8] S. Judd, *Photoelectric sensors and controls: Selection and application*. CRC Press, vol. 63, 1988.
- [9] P. Foster, Z. Sun, J. J. Park, and B. Kuipers, "Visagge: Visible angle grid for glass environments", in *Proceedings of the 2013 IEEE International Conference on Robotics and Automation (ICRA 2013)*, pp. 2213–2220, 2013.